Applied Surface Science 393 (2017) 309–315

Contents lists available at ScienceDirect

Applied Surface Science

journal homepage: www.elsevier.com/locate/apsusc

Full Length Article

Synthesis of graphene oxide and reduced graphene oxide by needle platy natural vein graphite

R.M.N.M. Rathnayake [a,c], H.W.M.A.C. Wijayasinghe [a,*], H.M.T.G.A. Pitawala [b], Masamichi Yoshimura [c], Hsin-Hui Huang [c]

[a] National Institute of Fundamental Studies, Kandy, Sri Lanka
[b] Department of Geology, University of Peradeniya, Peradeniya, Sri Lanka
[c] Graduate School of Engineering, Toyota Technological Institute, 2-12-1 Hisakata, Tempaku, Nagoya 468-8511, Japan

ARTICLE INFO

Article history:
Received 7 August 2016
Received in revised form
14 September 2016
Accepted 3 October 2016
Available online 5 October 2016

Keyword:
Needle platy graphite
Reduced graphene oxide
Graphene oxide
Chemical oxidation
Chemical reduction

ABSTRACT

Among natural graphite varieties, needle platy vein graphite (NPG) has very high purity. Therefore, it is readily used to prepare graphene oxide (GO) and reduced graphene oxide (rGO). In this study, GO and rGO were prepared using chemical oxidation and reduction process, respectively. The synthesized materials were characterized by X-ray diffraction (XRD), atomic force microscopy (AFM), scanning electron microscopy (SEM), high-resolution transmission electron microscopy (HRTEM), X-ray photoelectron spectroscopy (XPS), and Fourier transform infrared (FTIR) spectroscopy. XRD studies confirmed the increase of the interlayer spacing of GO and rGO in between 3.35 to 8.66 A°. AFM studies showed the layer height of rGO to be 1.05 nm after the reduction process. TEM micrographs clearly illustrated that the prepared GO has more than 25 layers, while the rGO has only less than 15 layers. Furthermore, the effect of chemical oxidation and reduction processes on surface morphology of graphite were clearly observed in FESEM micrographs. The calculated $R_{O/C}$ of GO and rGO using XPS analysis are 5.37% and 1.77%, respectively. The present study revealed the successful and cost effective nature of the chemical oxidation, and the reduction processes for the production of GO and rGO out of natural vein graphite.

1. Introduction

Natural graphite is an important raw material that can be used for many industrial applications [1,2]. At present, most of these industries still use expensive synthetic graphite, rather than natural graphite resources. This is possibly due to the fact that there is less awareness of the possibilities and practical procedures for the use of these natural resources. However, the recent studies carried out in the recent past revealed the possibility of producing high performing materials from natural graphite, or even as carbon-based nanomaterials, such as graphene oxide [2,3]. Among the countries possessing natural graphite resources, Sri Lanka is renowned for its highly crystalline vein graphite with high natural purity, in the range of 95–99% carbon. Therefore, there is a high potential for the production of different industrial products at low cost from these natural graphite resources [4,5]. The graphite has a hexagonal layered arrangement of carbon atoms in the crystal structure. In a plane, the C—C spacing is 1.42 A° and the planes are stacked in ABA Bernal stacking order with a layer distance of 3.34 A° [6]. In this crystalline structure, sp^2 hybridized carbon atoms are connected to each other by covalent bonds while the van der Waals interaction act between the adjacent planes [7]. This outer-plane weak interaction was allowed to slip on an adjacent plane in the presence of mechanical stress. This property has made the graphite suitable to use in many components which require high lubricating properties [7]. Furthermore, due to its hexagonal arrangement of carbon atoms the unhybridized *p*-orbitals can form an electron cloud throughout the lattice, which results in higher electrical conductivity. The electrical conductivity can reach 25,000 S/cm and in the range of 1000 S/cm for the plane of a single-crystal and dense polycrystalline graphite [7,8]. From this material, expanded graphite can be produced using a chemical oxidation process, and it is considered as a graphite intercalation compound [8–10]. Graphite can be expanded by the processes such as intercalation of strong acids with microwave irradiation, chemical oxidation and ultrasound irradiation [10,11]. In this study, expansion of graphite was carried out with a chemical oxidation technique, using 98% H_2SO_4, 85% H_3PO_4 and $KMnO_4$ [9]. This process is highly effective

* Corresponding author at: National Institute of Fundamental Studies, Hanatana road, Kandy, Sri Lanka.
E-mail addresses: athulawijaya@gmail.com, athula@ifs.ac.lk (H.W.M.A.C. Wijayasinghe).

http://dx.doi.org/10.1016/j.apsusc.2016.10.008
0169-4332/

to reduce the van der Waals interaction in between planes, which is inversely proportional to the interlayer spacing, thus increasing the interlayer distances [10]. A single layer of graphite has excellent mechanical, electrical, thermal and optical properties, and a high specific surface area. Chemically modified graphene (CMGs) and their colloidal suspensions allow them to be used in polymer composites, ultra-high capacitors, hydrogen storage materials, rechargeable batteries, conducting inks, thermal management, and chemical/biosensors [2,12].

Natural vein graphite can be categorized into four main structurally distinct varieties, which are namely: needle platy graphite (NPG); shiny slippery fibrous (SSF); coarse flake of radial (CFR); and coarse striated flaky (CSF) graphite [4,5]. Among these four varieties, NPG has the highest natural purity of around 99% [1]. NPG graphite typically exists in the mid-area of graphite veins and it can easily be separated manually.

While the production of graphene oxide (GO) and reduced graphene oxide (rGO) have been typically created from synthetic and flake graphite, high purity natural vein graphite has yet to be utilized fully. Therefore, the objective of the present study was to synthesize GO and rGO from high purity NPG variety of natural vein graphite by developing feasible and cost-effective methods.

2. Experimental

For the present study, improved Hummer's method was used to produce GO [3]. NPG variety of Sri Lankan vein graphite was used as the starting material. All the acids (98% H_2SO_4 and 85% H_3PO_4), oxidizing agents ($KMnO_4$ and 40% H_2O_2), 99.8% *N*,*N*-dimethylformamide (DMF) and 65% hydrazine monohydrate used for this study were purchased from Sigma-Aldrich.

Preparation of graphene oxide (GO) was carried out using chemical oxidation method, and for that 3 g of NPG were mixed with 18 g of $KMnO_4$, and 360 ml of 98% H_2SO_4 and 40 ml of 85% H_3PO_4 [9,13]. Then the mixture was stirred at 60 °C for 12 h and allowed to cool down to 30 °C. Then 4 ml of H_2O_2 was added into a separate beaker with 250 ml of deionized water and the prepared graphite mixture was added slowly into this beaker while stirring. The mixture was allowed to settle by keeping for six hours. Finally, the prepared sample was filtered and dried in a vacuum oven at 60 °C for 2 h [14,15]. Reduced graphene oxide (rGO) was prepared using 1 g of GO synthesized under the previous step. The GO sample was sonicated with 40 ml of *N*,*N*-dimethylformamide (DMF) for 1 h. Then it was stirred with 10 ml of hydrazine monohydrate at 80 °C for 12 h. Finally, the sample was washed with distilled water until the pH became 7 and then dried in a vacuum oven at 60 °C for 2 h.

The prepared materials were characterized by powder X-ray diffraction (XRD) (Rigaku-Ultima IV X-ray diffractometer) with a step size 0.02° and Cu Kα1 radiation to evaluate the expansion of graphite layers. The morphology of the samples was analyzed by atomic force microscope (AFM) (Nanoscope Multimode 8) with the silicon nitride cantilevers with the ring constant of 0.4 N/m. The surface of the samples was studied by EEVO/LS 15 ZEISS scanning electron microscopy (SEM). High-resolution transmittance electron microscopy (HRTEM) images were obtained by a JEM-2100 electron microscope, at an accelerating voltage of 200 kV. Specimens were prepared by dispersing powders in ethanol to form a suspension, and followed by ultrasonication for 1 h. The high-resolution images of periodic structures were analyzed and filtered by the fast Fourier transformation (FFT) method. The FTIR spectra were measured using Fourier transform infrared (FTIR) spectrophotometer (Nicolet 6700) with attenuated total reflectance to analyze functional groups attached to graphite surface. The elemental composition of the material surface was studied by PHI 5000 X-ray photoelectron spectroscopy (XPS) Al-Mg anode. The samples were dried in vacuum before obtaining measurements.

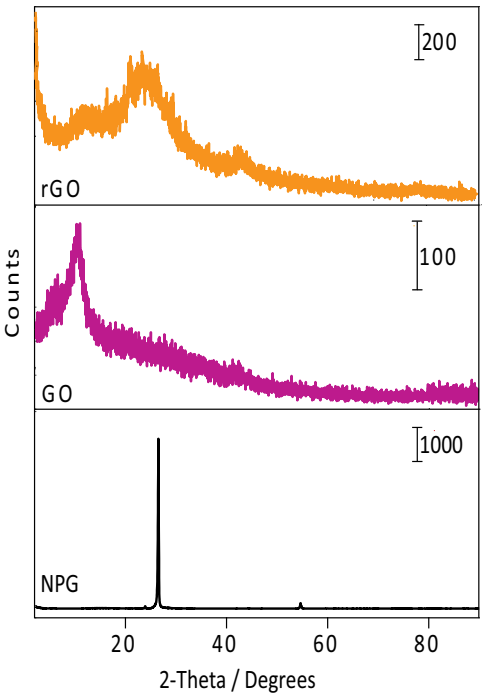

Fig. 1. X-ray diffractograms obtained on rGO, GO, and NPG.

3. Results and discussion

The X-ray diffractograms (XRD) obtained for NPG, GO, and rGO samples are shown in Fig. 1. The corresponding diffraction peaks were identified by comparing with the standard JCPDS data of graphite (JCPDS no. 23-64) [16,17].

The sharp diffraction peak appeared at $2\theta = 26.6$ A° of NPG vein graphite variety confirms the existence of graphite phase [17,18]. Further, the existence of a sharp, narrow peak with the absence of any residual phase seen in this diffractogram of NPG, indicates that this graphite is highly crystalline, and has very high purity, and lacks of mineral inclusions [19]. This can be due to the fact that the NPG is found in the middle part of the graphite vein. Thus, there is a high possibility for the existence of highly crystalline graphite with higher purity, because of less influence from the wall rock. Formation of GO leads to the expansion of graphite layers during the oxidation process [20–22]. Once the oxidation process is completed, the crystal structure has changed while oxygen-containing functional groups have been introduced into interlayers [23].

As seen in Fig. 1, the major peak of GO has shifted to the left compared to that of NPG, indicating an expansion of the interlayer space of graphite. It indicates that the method used in the present study can produce highly oxidized GO from NPG. Our resulted GO exhibits its major peak at $2\theta = 10.23°$ with the interlayer spacing of 0.866 nm of (*001*) plane [21,23,24]. This major peak is a board peak typical to GO and this type of peak broadening in the diffractograms can be observed in GO and rGO, due to the decrease of the crystal size into the nanoscale during the synthesis process. Further, in the X-ray diffractogram of the rGO sample, the main diffraction peak appears at $2\theta = 25.36°$ with a corresponding interlayer spacing of 0.350 nm. It indicates a successful reduction of GO into rGO. This broad peak indicated that the rGO nanosheets are exfoliated into a monolayer or of few layers of rGO and resulted in a new lattice structure which is significantly different from the NPG and GO [18,25]. These results indicate that the pre-exfoliation of vein graphite directed to the dif-

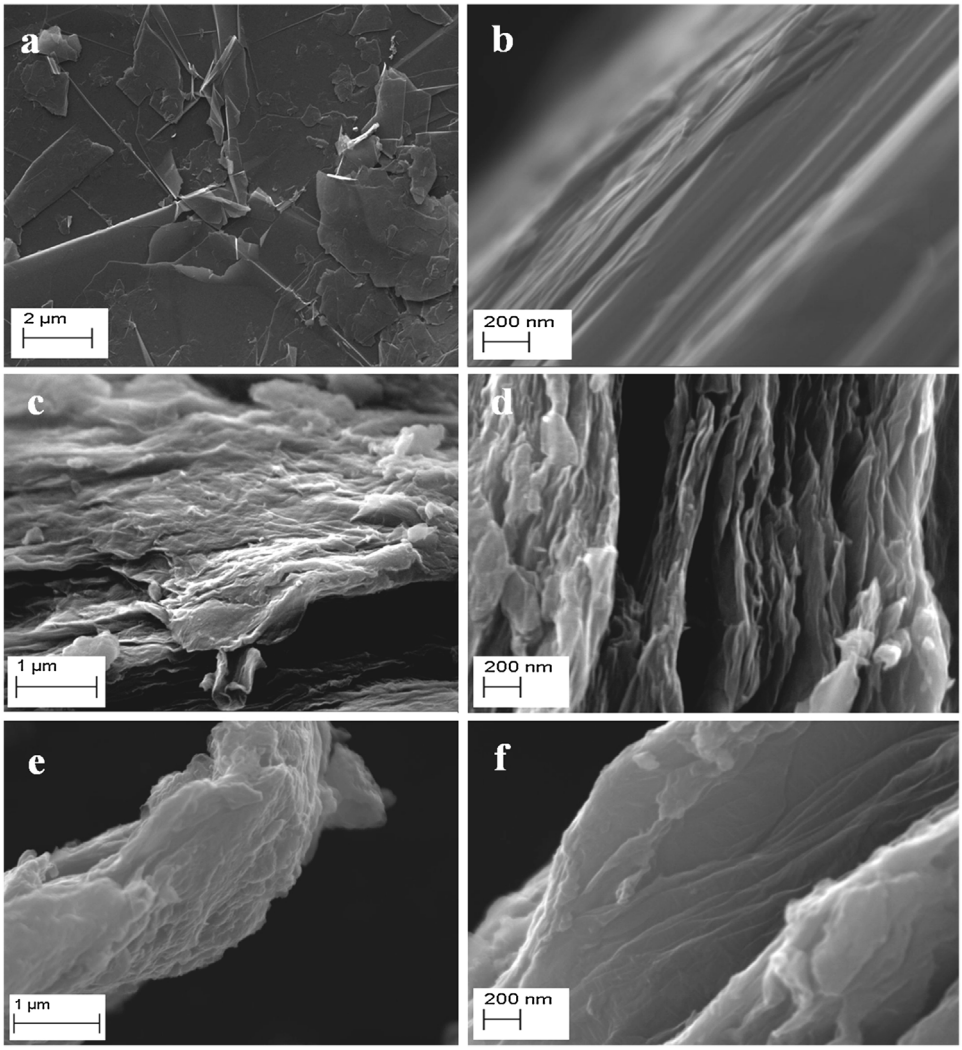

Fig. 2. FESEM micrographs of NPG and the synthesized products at different magnifications (a), and (b) from NPG, (c) and (d) from GO and, (e) and (f) from rGO.

ferent interlayer spacing for GO is possibly due to the difference in the content of intercalated oxide functional groups [18,25].

The FESEM micrographs show (Fig. 2) the morphological differences between NPG, GO, and rGO. The layer stacking of NPG is not well distinguished, may be due to the densely packed planes. Further, it is seen that the graphite particles have very sharp edges and smooth surfaces in their raw form (Fig. 2(a) and (b)).

As discussed under the XRD study above, the different d-spacing of GO depends on the degree of oxidation. After the chemical oxidation, the layer distance enlarges and GO will crimp, while the interlayer Vander-Waal force reduced [22,26]. The TEM image of GO shown in Fig. 4(b) will also give evidence for the existence of this crimp like structure in GO. As shown in Fig. 2(c) and (d), the GO synthesized in this study shows a loosely bonded nature. Also, the FESEM micrographs (Fig. 2) obtained on the synthesized rGO show a further expansion of the layers and the sharp edges present in graphite has disappeared during the oxidation process and all edges have become smoother. The GO prepared in this study shows some distinct changes in the physical appearance, especially the GO surface appears more puffed and shrunken.

The FESEM images of rGO given in Fig. 2(e) and (f) shows separation of layers into a few number of sheets with a flower petal-like appearance. Generally, rapidly build up thermal vibrations divert the nanoparticles into the micron scale, and changes the two-dimensional (2D) crystallites into a variety of stable 3D structures [27]. Accordingly, rGO layers are naturally crumpled and flexible, in contrast to graphite [26,27]. FESEM images of the rGO show (Fig. 2(e) and (f)) detached thin layers. This detached and folded appearance of thin layers of rGO further be seen in the TEM images shown in Fig. 4(c) and (d). However, they occur as aggregates of fine particles formed during the reduction process.

AFM was used to clarify the lateral dimension, layer thickness and the topographical features of the GO and rGO. This study was carried out in air using silicon nitride cantilever. A drop from GO and the rGO dispersion was cast on a silicon substrate and allowed to dry completely in air for 30 min, in which a small amount of dust presented on the surface as seen in the bright spots in Fig. 3(a) and (b). Cross-sectional analysis of the AFM micrographs indicates the presence of individual sheets of GO with a layer thickness of around 1.2 nm which corresponds to a single layer of GO (Fig. 3(a)).

Fig. 3(b) shows the AFM image of rGO, which displays plenty of individual graphene sheets with an average layer thickness of 1.05 nm, corresponds to a single layer graphene. However, when compared to GO, the synthesized rGO shows a wrinkled and aggregated nature with very low layer thickness, which may be due to the differences in exfoliation behavior and other factors [28]. The height of GO is not constant, however, and the carbon layers in GO consist of two kinds of states, aromatic regions with unoxidized benzene rings and aliphatic regions with six-membered carbon rings [21,28]. However, the degree of oxidation is propor-

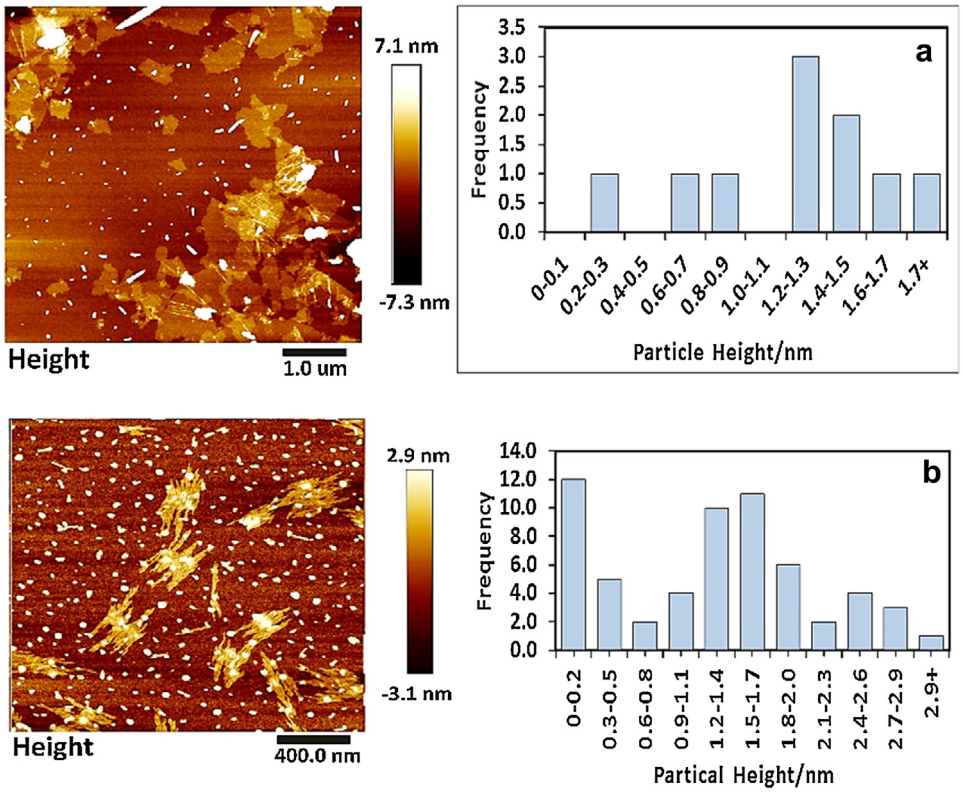

Fig. 3. AFM micrographs of (a) GO and (b) rGO.

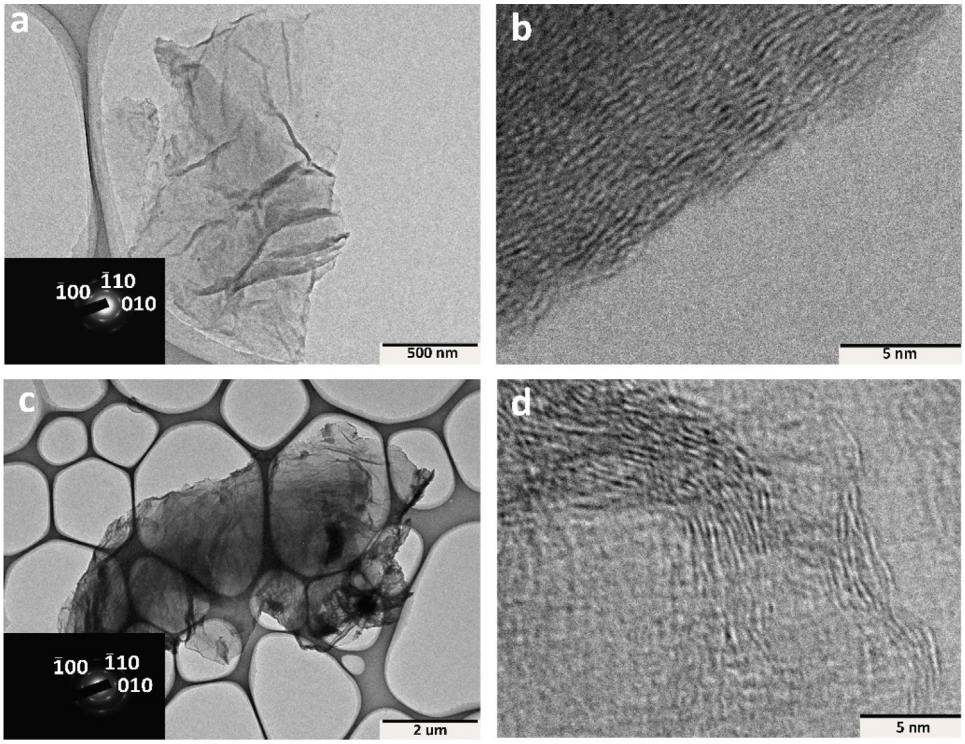

Fig. 4. Low-magnification bright-field TEM images of (a) GO and (c) rGO specimens with insets of corresponding [0001] electron diffraction patterns. (b), and (d) TEM images of the folded edges of GO and rGO, respectively.

tional to the number of hydrophilic sites present in the basal plane of graphite [28,29]. It should be noted that the spider-like feature (different from the SEM images) might be related to the sample preparation method, where small rGO sheets shrink while drying.

The morphology and crystal structure of the GO and rGO were investigated by transmission electron microscopy (TEM), and the results are shown in Fig. 4. The GO sample shows a wrinkled surface, caused by the overlapping sheets. On the other hand, the rGO

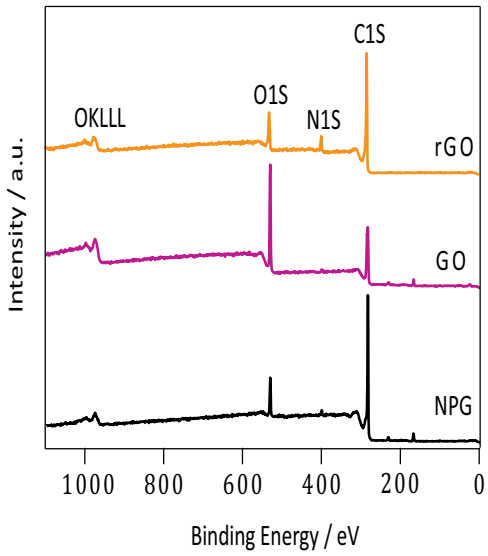

Fig. 5. XPS survey spectra of NPG graphite, GO and r GO.

Table 1
Atomic concentrations of O1s, C1s and their ratios obtained by XPS survey spectra.

Sample ID	Elements (at%)		O/C ratio
	O1s	C1s	
NPG	2.31	97.44	0.23
GO	33.89	63.09	5.37
rGO	13.99	78.77	1.77

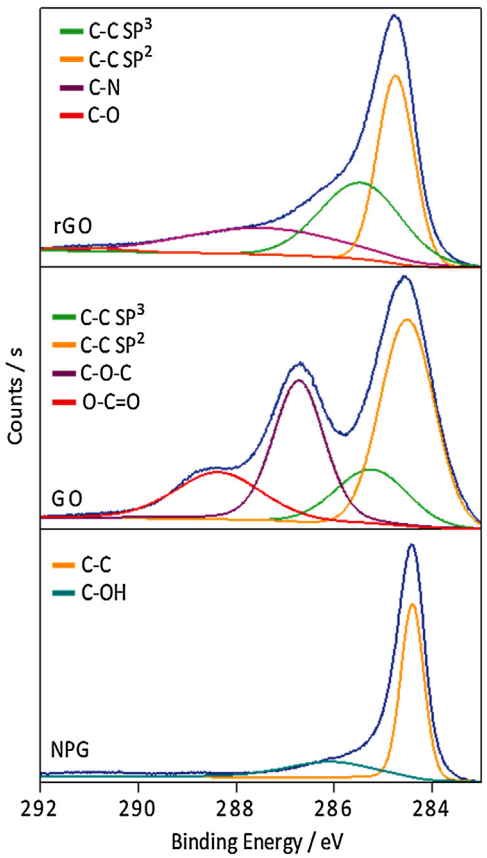

Fig. 6. C1s core level XPS spectra of NPG, GO, and rGO.

sample exhibits a rather wavy and crumbled structure, which is consistent with the SEM results. The size of the sheets is in the ranges from 1.1 to 2 μm for GO and 2 to 8.5 μm for rGO. The Insets in Fig. 4(a) and (c), correspond to the (001) selected-area electron diffraction (SAED) patterns.

Both of the prepared GO and rGO show six-fold symmetry diffraction spots, indicating the crystallinity in nature. Note that these diffraction patterns were acquired in an area of 1.5 μm in diameter. The lattice parameters of GO and rGO were measured to be 0.232 ± 0.003 nm and 0.249 ± 0.053 nm, respectively, which are almost the same as reported in the literature [15,21]. To quantify the number of layers in graphite/graphene, the number of folds at the edge of the flakes/sheets in high-resolution TEM images [(HRTEM) (Fig. 4(b) and (d))] were counted [23]. It was counted to be more than 25 layers for GO, while rGO has less than 15 layers. Again, these results can be correlated to its exfoliation behavior and matched with the results obtained under the XRD study.

X-ray photoelectron spectroscopy is a facile and effective quantitative method to determine the elemental composition of a material surface. The XPS spectrum obtained on the synthesized GO indicates the level of oxidation relative to the level of organic functional groups attached to a graphite structure [8,14]. The survey 1s (Su1s) spectrum of GO represents (Fig. 5) the presence of carbon, oxygen, nitrogen and sulfur containing functional groups in the prepared GO material. Table 1 shows the atomic concentrations of O1s, C1s and their ratios for all the samples. It was found that NPG contains 2.31% of oxygen, and after the chemical oxidation, the oxygen concentration increased up to 33.89% along with the reduction of the carbon content [14,30]. Also, it was clearly seen that the ratio of oxygen to carbon concentration increased from 0.23% to 5.37% during the chemical oxidation of graphite. This results clearly suggest that the chemical oxidation process exfoliated the vein graphite and a large amount of oxygen functional groups were introduced on the surface of the vein graphite. However, the oxygen concentration was reduced up to 13.99% after the reduction of GO into rGO. Further, the ratio of oxygen to carbon concentrations was decreased from 5.32% to 1.77% during the chemical reduction. In order to identify the different functional groups, which were formed on the graphite surface, on either the basal or the edge plane during the chemical oxidation and reduction process, de-convolution of the high level of C1s core level spectra of NPG, GO, and rGO samples were carried out and results are presented in Fig. 6. The de-convolution of C1s spectra into different binding energies (B.E.) with their peak assignments are summarized in Table 2.

The C1s spectrum of GO (Fig. 6) corresponds to five bands, which correspond to the functional groups of: carbon Sp^2 (C=C, 284.05); carbon Sp^3 (C—C, 284.70); ether (C—O—C, 285.50); carbonyl (C=O, 286.13); and carboxylates (O—C=O, 288.65) [14,16,24]. But, after

Table 2
XPS analysis summary of the binding energy observed in C1s spectra for graphite, GO, and rGO samples.

Sample ID	C1s peak assignment with corresponding B.E (eV)						
	C—C/Sp2	C—C/Sp3	C—O—C	O—C=O	C=O	C—O	C—N
NPG	284.30	284.4	285.34	–	286.17	–	–
GO	284.05	284.7	285.5	288.65	286.13	–	–
rGO	284.68	285.45	–	–	–	290.15	287.38

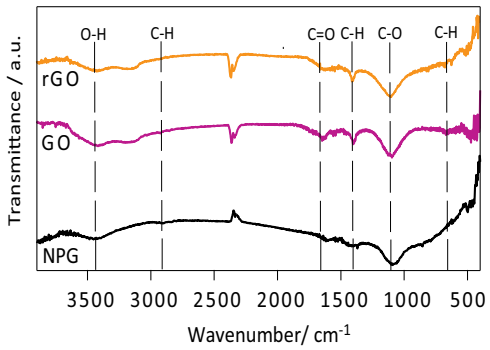

Fig. 7. FTIR spectra of NPG, GO, and rGO.

the reduction process, the Sp^2 peak of GO (Fig. 6) disappeared, and the O1s peak reduced significantly [30].

The XPS spectra of the rGO (Fig. 6) shows peaks at 284.68 eV, 285.45 eV, 287.38 eV and 290.15 eV corresponds to the C—C Sp^2, C—C—Sp^3, C—N, and C—O, respectively [8,16]. The peak position belonging to the C—N bond corresponds to the excess of hydrazine present in the freshly prepared rGO [8]. They are referenced by to the Nitrogen atom, which is located into the π conjugated system and contributes to the π system with one or two *p*-electron [8,14]. The functional groups obtained from de-convoluted core level C1s spectra of GO and rGO are consistent with the results obtained from FTIR analysis. Considering the FTIR and XPS analysis of both materials, it further confirmed the formation of a significant structure for both GO and rGO.

The peak C1s is higher than the O1s peak of rGO (Fig. 6). This indicates that the restoration of the rGO can be achieved by the increase of Sp^2 carbon content [20]. The oxygen to carbon ratio was determined from the C1s atomic concentration values in both GO and rGO [27]. The chemical reduction of hydrazine acts as a heteroatom and is highly effective for removing the oxygen functional groups, which tend to remain covalently bonded to the surface of the rGO in the form of hydrazine [16].

The Furrier transform infrared (FTIR) spectra given in Fig. 7 shows a weak absorption peak around V_{max}/cm^{-1} 674.1 corresponding to the bending of the aromatic C—H bond. The medium weak absorption around V_{max}/cm^{-1} 1642.1 is related to aromatic C=C stretching bonds present in the graphite. Also, according to the hybridization present in the graphite doubly splits peak around V_{max}/cm^{-1} 2300–2400 are related to the stretching of Sp^3 and Sp^2 hybridized C—H bonds present in graphite [8].

The FTIR spectrum of synthesized GO is shown in Fig. 7. When the FTIR spectra of GO is compared with that of NPG, a strong peak can be seen near V_{max}/cm^{-1} 1120, which corresponds to the C—O stretching vibration. It is an indication of alcohols, carboxylic acids, esters, or ethers. In these experimental conditions, it could possibly be of alcohols or carboxylic functional groups. Also, several new strong peaks are present between V_{max}/cm^{-1} 1650 and 1750, which are in the wave number region of C=O stretching vibration. This is an indication of the presence of carbonyl groups. Also, several other strong peaks can be seen between V_{max}/cm^{-1} 3600–3800, which are related to the O—H stretching or free hydroxyl units. It is an indication of alcohol or phenol functional groups present in prepared GO sample. The peaks present in FTIR spectra of NPG graphite (Fig. 7) around 1600 cm^{-1} are also present in the FTIR spectra of GO. These peaks are in the wave number region of C—C stretching (in–ring) vibrations and they represent non-oxidized carbon rings. It indicates the incomplete oxidation of graphite.

As for the structure of rGO, it has the two resonance structures; diene and dienophile. Fig. 7 shows the FTIR spectra of reduced graphene oxide (rGO) prepared by GO. Here the synthesized materials show the existence of weak peaks in the range of V_{max}/cm^{-1} 650–800, which indicate the presence of variable bending absorption of aromatic C—H. The rGO has a major peak when compared to graphite and GO, and it lies between V_{max}/cm^{-1} 1450–1600 [8].

4. Conclusion

This study presented preparation of novel material of graphene oxide (GO) and reduced graphene oxides (rGO) based on high purity highly crystalline but low-cost needle platy (NPG) variety of natural vein graphite. It is revealed here that the modified chemical oxidation and the reduction methods as effective processes for the production of GO and rGO from the selected natural vein graphite. The interlayer spacing of the synthesized GO is relatively large, due to more oxygenated functional groups introduced to the carbon surface, which confirmed the formation of GO. The morphological studies conducted using AFM, FESEM and HRTEM show a packed sheet-like morphology of NPG vein graphite turned into exfoliated grains during the oxidation process. The oxygen content increased with the oxidation without distortion of the lattice structure was also confirmed from HRTEM and SAED patterns. Furthermore, XPS and FTIR analyses predict the degree of oxidation of NPG vein graphite during oxidation and reduction, whereas the oxygen bonded carbon component increased during the chemical oxidation and decreased during the chemical reduction of GO. Altogether this study shows the ability to prepare high quality, few-layer GO and rGO by using high purity highly crystalline but cheaper natural vein graphite.

Acknowledgements

This work was supported by the National Institute of Fundamental Studies, Sri Lanka and Graduate School of Engineering, Toyota Technological Institute, Japan.

References

[1] H.P.T.S. Hewathilake, N.W.B. Balasooriya, H.M.T.G.A. Pitawala, H.W.M.A.C. Wijayasinghe, Use of crystal morphologies to unravel the origin of vein graphite in Sri Lanka, J. Geol. Soc. Sri Lanka 17 (2015) 65–73.
[2] N.W.B. Balasooriya, P.H. Touzain, P.W.S.K. Bandaranayake, Capacity improvement of mechanically and chemically treated Sri Lanka natural graphite as an anode material in Li-ion batteries, Ionics 13 (2007) 305–309.
[3] A.R. Kumarasinghe, L. Samaranayake, F. Bondino, E. Magnano, N. Kottegoda, E. Carlino, U.N. Ratnayake, A.A.P. de Alwis, V. Karunaratne, G.A.J. Amaratunga, Self-assembled multilayer graphene oxide membrane and carbon nanotubes synthesized using a rare form of natural graphite, J. Phys. Chem. C 117 (2013) 9507–9519.
[4] K.V.W. Kehelpannala, Epigenetic vein graphite mineralization in the granulite terrain of Sri Lanka, Gondwana Newslett. 2 (1999) 654–657.
[5] P. Touzain, N. Balasooriya, K. Bandaranayake, C. Descolas-Gros, Vein graphite from the Bogala and Kahatagaha-Kolongaha mines, Sri Lanka: a possible origin, Can. Mineral. 48 (2010) 1373–1384.
[6] J.W. McClure, Band structure of graphite and de Haas-van Alphen Effect, Phys. Rev. 108 (1957) 612–618.
[7] X.J. Lu, E. Forssberg, Preparation of high-purity and low-sulphur graphite from Woxna fine graphite concentrate by alkali roasting, Miner. Eng. 15 (2002) 755–757.
[8] C. Zhang, W. Lv, X. Xie, D. Tang, C. Liu, Q.-H. Yang, Towards low temperature thermal exfoliation of graphite oxide for graphene production, Carbon 62 (2013) 11–24.
[9] W.W. Focke, H. Badenhorst, W. Mhike, H.J. Kruger, D. Lombaard, Characterization of commercial expandable graphite fire retardants, Thermochim. Acta 584 (2014) 8–16.
[10] M. Cai, D. Thorpe, D.H. Adamson, H.C. Schniepp, Methods of graphite exfoliation, J. Mater. Chem. 22 (2012) 24992–25002.
[11] J. Li, J. Li, M. Li, Ultrasound irradiation prepare sulfur-free and lower exfoliate-temperature expandable graphite, Mater. Lett. 62 (2008) 2047–2049.
[12] Z. Ying, X. Lin, Y. Qi, J. Luo, Preparation and characterization of low-temperature expandable graphite, Mater. Res. Bull. 43 (2008) 2677–2686.
[13] Y.-p. Chen, S.-y. Li, R.-y. Luo, X.-m. Lv, X.-j. Wang, Optimization of initial redox potential in the preparation of expandable graphite by chemical oxidation, New Carbon Mater. 28 (2013) 435–441.

[14] D.C. Marcano, D.V. Kosynkin, J.M. Berlin, A. Sinitskii, Z. Sun, A. Slesarev, L.B. Alemany, W. Lu, J.M. Tour, Improved synthesis of graphene oxide, ACS Nano 4 (2010) 4806–4814.
[15] A. Vesel, A. Drenik, M.B. Pichelin, M. Passarelli, M. Mozetic, Oxidation of graphite with neutral oxygen atoms at elevated temperature, in: 35th EPS Conference on Plasma Phys., Hersonissos, 2008, pp. 1.014.
[16] D.R. Dreyer, S. Park, C.W. Bielawski, R.S. Ruoff, The chemistry of graphene oxide, Chem. Soc. Rev. 39 (2010) 228–240.
[17] J.-Z. Wang, L. Lu, M. Choucair, J.A. Stride, X. Xu, H.-K. Liu, Sulfur-graphene composite for rechargeable lithium batteries, J. Power Sour. 196 (2011) 7030–7034.
[18] X. Cheng, H. Liu, Q. Chen, J. Li, P. Wang, Preparation of graphene film decorated TiO2 nano-tube array photoelectrode and its enhanced visible light photocatalytic mechanism, Carbon 66 (2014) 450–458.
[19] M. Kędzierski, P. Jankowski, G. Jaworska, A. Niska, Graphite oxide as an intumescent flame retardant for polystyrene, Polimery 57 (5) (2012) 347–353.
[20] S. Sheshmani, M.A. Fashapoyeh, Suitable chemical methods for preparation of graphene oxide, graphene and surface, Acta Chim. Slovenica 60 (2013) 813–825.
[21] G. Zhao, T. Wen, C. Chen, X. Wang, Synthesis of graphene-based nanomaterials and their application in energy-related and environmental-related areas, RSC Adv. 2 (2012) 9286–9303.
[22] Y. Zhu, S. Murali, W. Cai, X. Li, J.W. Suk, J.R. Potts, R.S. Ruoff, Graphene and graphene oxide: synthesis, properties, and applications, Adv. Mater. 22 (2010) 3906–3924.
[23] P. Dash, T. Dash, T.K. Rout, A.K. Sahu, S.K. Biswal, B.K. Mishra, Preparation of graphene oxide by dry planetary ball milling process from natural graphite, RSC Adv. 6 (2016) 12657–12668.
[24] Long-Yue Meng, Soo-Jin Park, Characterization of reduced graphene nanosheets viaPre-exfoliation of graphite flakes, Bull. Korean Chem. Soc. 33 (2012) 209–214.
[25] Z. Gao, J. Wang, Z. Li, W. Yang, B. Wang, M. Hou, Y. He, Q. Liu, T. Mann, P. Yang, M. Zhang, L. Liu, Graphene nanosheet/Ni2+/Al3+ layered double-hydroxide composite as a novel electrode for a supercapacitor, Chem. Mater. 23 (2011) 3509–3516.
[26] S. Park, R.S. Ruoff, Chemical methods for the production of graphenes, Nat. Nano 4 (2009) 217–224.
[27] S. Stankovich, D.A. Dikin, R.D. Piner, K.A. Kohlhaas, A. Kleinhammes, Y. Jia, Y. Wu, S.T. Nguyen, R.S. Ruoff, Synthesis of graphene-based nanosheets via chemical reduction of exfoliated graphite oxide, Carbon 45 (2007) 1558–1565.
[28] W.W. Focke, H. Badenhorst, S. Ramjee, H.J. Kruger, R. Van Schalkwyk, B. Rand, Graphite foam from pitch and expandable graphite, Carbon 73 (2014) 41–50.
[29] S. Stankovich, D.A. Dikin, G.H.B. Dommett, K.M. Kohlhaas, E.J. Zimney, E.A. Stach, R.D. Piner, S.T. Nguyen, R.S. Ruoff, Graphene-based composite materials, Nature 442 (2006) 282–286.
[30] Z.W.X.J. Yanzhong Hong, Sulfuric acid intercalated graphite oxide for graphene preparation, Sci. Rep. 3 (2013) 3439.